Simple v approximation for optimization of debris-to-debris transfers

Simple ΔV Approximation for Optimization of Debris-to-Debris Transfers

Hong-Xin Shen [1]
Xi'an Satellite Control Center, 710043 Xi'an, China

Lorenzo Casalino [2]
Politecnico di Torino, 10129 Torino, Italy

Nomenclature

a = semi-major axis, km

e = eccentricity

i = inclination, rad

J_2 = Earth's first zonal harmonic

M = mean anomaly, rad

r_E = Earth's equatorial radius, km

s_x = coefficient of x

s_y = coefficient of y

s_z = coefficient of z

t = time, s

v = velocity, km/s

x = velocity change for node change, km/s

y = velocity change for semi-major axis change, km/s

z = velocity change for inclination change, km/s

δa = semi-major axis change, km

δi = inclination change, rad

$\delta\dot{\Omega}$ = change of $\dot{\Omega}$, rad/s

Δv = velocity change, m/s

[1] Assistant Professor, State Key Laboratory of Astronautic Dynamics; hongxin.shen@gmail.com.
[2] Associate Professor, Dipartimento di Ingegneria Meccanica e Aerospaziale, Corso Duca degli Abruzzi, 24; lorenzo.casalino@polito.it.

Δe = eccentricity change

μ = Earth's gravitational parameter, km^3/s^2

Ω = right ascension of ascending node, rad

$\dot{\Omega}$ = right ascension of ascending node rate, rad/s

ω = argument of perigee, rad

subscript

k = debris number

E = Earth

a = initial impulse

b = final impulse

e = eccentricity correction for velocity change

I. Introduction

A large number of space debris occupies the Earth orbit regions of most interest, mainly in low-Earth orbit (LEO) and geostationary orbit (GEO). Operational satellites and manned space vehicles or stations are threatened to be destroyed by space debris. Kessler Syndrome [1] states that more and more debris might be produced due to collision events, even if all launches into space stopped immediately. Active debris removal (ADR) of existing large objects from orbit is the only remediation of the debris presence in the near-Earth environment, in order to avoid future problems for space research and commercialization [2]. Recent studies have led to the conclusion that, in addition to mandatory end-of-life disposal of new satellites, removing about 5 objects per year may be necessary to stabilize the future LEO debris population [3].

The LEO debris population is characterized by several clusters of objects, which occupy orbits with similar altitude (but not exactly the same) at particular inclinations, that is, the most useful for space applications (e.g., Sun-synchronous, Molniya). However, the orbital planes of objects in a cluster do not coincide, as Earth oblateness perturbs the right ascension of ascending node (RAAN). Each object has in general a different RAAN rate of change, as this effect depends on its orbital elements (mainly, the semi-major axis and the inclination). As a consequence, RAAN values in a cluster are typically spread almost uniformly between 0 and 360 degrees. By using Earth

oblateness perturbation, efficient sequences of debris objects with limited transfer costs can be found by exploiting the differential nodal precession rates, in order to define low cost ADR mission for the removal of multiple objects.

In a typical scenario, an active debris removal spacecraft performs rendezvous with the target and delivers a deorbiting kit, which then provides a velocity change to the debris object and places it on a reentry trajectory. There is an obvious advantage if the same ADR mission can remove more than a single object. In efficient mission architectures, the chaser, after rendezvous, attaches a deorbiting kit to each target and then moves towards the following object. The choice of the targets and removal sequence is crucial to the cost-effectiveness of such missions. The sequence optimization results in a combinatorial problem, which has been studied using approaches such as branch and bound algorithms [4], ant colony optimization [5], column generation techniques [6].

Large combinatorial problems suffer from the dimensionality curse, and it is essential to analytically estimate the body-to-body transfer cost, in order to enable the exploration of broad search spaces in a reasonable computational time. Previous works generally estimated the transfer Δv by adding or taking the root-sum-square of the individual Δvs needed to match the semi-major axis, node angle, and inclination of the target debris [7]. Alfriend et al. presented an analytical estimation for satellite-to-satellite transfer in order to get an optimal servicing of multiple targets, but the focus was on Geosynchronous orbits [8], where J2 has a negligible effect.

Machine learning has attracted extensive interest in the last decade and may have significant influence to various researches of aerospace engineering [9]. Recent works [10][11] explore the capabilities of deep neural networks to improve fast estimation of impulsive transfers, obtaining a mean relative error of less than 4%, but one has to balance the advantage of computation speed against remarkable time for datasets generating and network training.

When considering the RAAN match in LEO for a specified transfer time, the general strategy consists in waiting for RAAN drift to align the orbit planes. However, in many circumstances this strategy may not be feasible because the waiting time can be very large. In this paper, a simple analytical method is developed to accurately approximate the transfer costs between two objects of the removal sequence. The accuracy of these estimations is verified by comparison with existing optimized solutions. Rendezvous transfers between two given orbits are dealt with using an accurate dynamical model that takes J2 perturbation into account. The state-of-the-art solution winner of the ninth Global Trajectory Optimization Competition (GTOC9) by JPL [12] is used as benchmark to verify the accuracy of the method presented in this paper.

II. Dynamic model

Space debris dynamics is usually defined by a set of Two-line Elements (TLE), which are propagated with the SGP4 model [13]. However, the model accuracy degrades with time, and the TLE information has to be updated regularly. A simplified propagation model is adopted in this paper to describe the dynamics of the debris.

The body orbit is described by means of osculating orbital elements, which are specified at the known ADR mission departure time. Targets for removal missions have relatively large values of semi-major axis and small eccentricity, as aerodynamic drag would otherwise cause a fast natural orbit decay. Therefore, this paper considers only objects with these characteristics, and atmospheric drag is here neglected. Only secular orbit perturbation due to Earth oblateness (related to the harmonic term J2) is then considered. Semi-major axis *a*, eccentricity *e* and inclination *i* are constant, whereas right ascension of ascending node Ω, argument of periapsis ω and mean anomaly *M* vary according to

$$\frac{\mathrm{d}\Omega}{\mathrm{d}t} = -\frac{3}{2}\sqrt{\frac{\mu}{a^3}}\frac{J_2\cos i}{\left(1-e^2\right)^2}\left(\frac{r_E}{a}\right)^2 \tag{1}$$

$$\frac{\mathrm{d}\omega}{\mathrm{d}t} = \frac{3}{4}\sqrt{\frac{\mu}{a^3}}\frac{J_2\left(5\cos^2 i-1\right)}{\left(1-e^2\right)^2}\left(\frac{r_E}{a}\right)^2 \tag{2}$$

$$\frac{\mathrm{d}M}{\mathrm{d}t} = \sqrt{\frac{\mu}{a^3}} + \frac{3}{4}\sqrt{\frac{\mu}{a^3}}\frac{J_2\left(3\cos^2 i-1\right)}{\left(1-e^2\right)^{3/2}}\left(\frac{r_E}{a}\right)^2 \tag{3}$$

where μ is Earth's gravitational parameter, r_E is Earth's equatorial radius.

By differentiating Eq. (1), one obtains the RAAN rate change ($\delta\dot{\Omega}$) caused by small changes of *a* (δa) and *i* (δi)

$$\frac{\delta\dot{\Omega}}{\dot{\Omega}} = -\frac{7}{2}\frac{\delta a}{a} - \tan i\,\delta i \tag{4}$$

When the initial values of orbital elements are given, the perturbed values can therefore be evaluated at any time *t*, and position and velocity are consequently determined. This simplified propagation model has been compared to the SGP4 propagator [5]. Orbit shape and orientation show good accuracy even for 200-day propagation (errors below few kilometers). Larger errors are found for argument of perigee and mean anomaly, but these discrepancies have a limited impact on the transfer costs. The eccentricity is small and ω differences have little effect, whereas

phase adjustments can be obtained with small Δv, as a large number of revolutions are typically required during each transfer leg. Thus, the propagation accuracy is considered to be satisfactory.

III. Approximate Transfer Cost Evaluation

In the scenario considered here, the launcher inserts the chaser spacecraft into rendezvous conditions with one of the objects in the debris set (target 1), and the removal kit is delivered. The mission starts at initial time t_1=0 and the chaser orbital elements are those of the initial object at t_1. The chaser then maneuvers to perform rendezvous with the following target and so on, until the last object has been reached. The present work focuses on finding a way to estimate the transfer cost between objects pairs as a function of transfer time, in order to speed up the performance of combinatorial optimization algorithms that define the best object sequences.

An optimal transfer time, which minimizes the propellant consumption, exists for any debris pair. The most favorable opportunities occur only when the required plane change is small, and therefore when the RAAN of the chaser is equal (or, at least, sufficiently close) to that of the target. The chaser can remain on its initial orbit until the favorable orbit alignment is achieved, and then perform a relatively short Hohmann-like transfer. Mission designers can take advantage of J2 perturbation, which changes the RAAN of bodies orbiting the Earth with a rate that depends on semi-major axis and inclination. Objects with different orbits will therefore have different rates of change of Ω, meaning that RAANs of two objects will become equal at a specific time, thus enabling the optimal transfer. However, cases when this kind of solutions are not suitable may occur, e.g., in the presence of strict time constraints, and an estimation method capable of dealing with non-optimal transfer time is required.

The impulse to simultaneously change velocity magnitude (i.e., semi-major axis) and orbit plane (i.e., RAAN and inclination) can be written as:

$$\Delta v = \sqrt{v_1^2 - 2v_1 v_2 \cos\vartheta + v_2^2} \tag{5}$$

where v_1 and v_2 are the velocity before and after the impulse and ϑ is the angle between them. For small plane changes one has [14]:

$$\vartheta = \sqrt{\left(\Delta\Omega \sin i\right)^2 + \Delta i^2} \tag{6}$$

Eq. (5) can be rewritten as

$$\Delta v = \sqrt{v_1^2 \sin^2\vartheta + v_1^2 \cos^2\vartheta - 2v_1 v_2 \cos\left(\vartheta\right) + v_2^2} \tag{7}$$

which further reduces to

$$\Delta v = \sqrt{v_1^2 \sin^2 \vartheta + \left(v_1 \cos \vartheta - v_2\right)^2} \tag{8}$$

For a small value of ϑ, $\sin \vartheta \approx \vartheta$, $\cos \vartheta \approx 1$; moreover, $v_2 - v_1 \approx -0.5 v_0 \Delta a / a_0$ can be related to the change of semi-major axis, and Eq. (8) is rewritten as

$$\Delta v = \sqrt{\Delta v_{\text{sa}}^2 + \Delta v_i^2 + \Delta v_\Omega^2} \tag{9}$$

This root-sum-square form can be seen as a simple approximation of Eq. (5), where $\Delta v_{\text{sa}} = 0.5 v_0 \Delta a / a_0$, $\Delta v_i = v_0 \Delta i$, and $\Delta v_\Omega = v_0 \Delta\Omega \sin i_0$ are the required velocity changes due to semi-major axis, inclination and RAAN, respectively. Subscript 0 relates to the average value between the initial and final orbits.

A. The transfer time is optimal

The optimal arrival time from debris *k* to *k*+1 can be easily evaluated, given differences of initial RAAN and RAAN rate of change

$$t_{\text{opt}} = \frac{\Omega_k \left(t = 0\right) - \Omega_{(k+1)} \left(t = 0\right) + 2K\pi}{\dot{\Omega}_{(k+1)} - \dot{\Omega}_k} \tag{10}$$

where the integer value of *K* that correspond to the first opportunity ($t_{\text{opt}} > t_{\text{k}}$) can be selected.

Optimal phasing is assumed to obtain an estimation of the transfer Δv. Equation (9) is empirically modified to account for the additional change of eccentricity vector Δe (in addition to semi-major axis and inclination) [15]:

$$\Delta v / v = \sqrt{\left(0.5 \Delta a / a\right)^2 + \Delta i^2 + \left(0.5 \Delta e\right)^2} \tag{11}$$

The average value of semi-major axis *a* of the two objects involved in the leg, and the corresponding circular velocity *v* are used.

According to the above analysis, the optimal trip time and the corresponding velocity change between any debris pair can be determined. It is worth noting that a change of arrival time for leg *k* usually does not propagate to the following legs, as convenient transfers typically require relatively long waiting times before starting to maneuver. This approximation has been validated with good accuracy, as shown in a previous work [5].

B. The transfer time is limited

The arrival time from debris *k* to *k*+1 is imposed as $t_{k+1} < t_{opt}$. Eq. (1) provides the final difference of RAAN between the chaser and the target. It is assumed that $\Omega_{k+1}\left(t_{k+1}\right) - \Omega_k \left(t_{k+1}\right) \neq 0$, $a_{k+1} - a_k \neq 0$, $i_{k+1} - i_k \neq 0$; the

quantities *x*, *y*, *z*, are defined in order to account for the required Δv cost corresponding to the changes of RAAN, semi-major axis, and inclination, respectively :

$$x = \left(\Omega_{k+1}\left(t_{k+1}\right) - \Omega_k\left(t_{k+1}\right)\right)\sin i_0 v_0 \tag{12}$$

$$y = \frac{a_{k+1} - a_k}{2a_0} v_0 \tag{13}$$

$$z = \left(i_{k+1} - i_k\right) v_0 \tag{14}$$

where $a_0 = \left(a_{k+1} + a_k\right)/2$, $i_0 = \left(i_{k+1} + i_k\right)/2$, and $v_0 = \sqrt{\mu / a_0}$.

A two-impulse transfer is considered in this approximate analysis. Without loss of generality, the first impulse completes a partial change of *x*, *y*, *z*, (s_x, s_y, and s_z are the respective fractions) and the second impulse makes up the remaining difference. It is worth noting that the fuel-saving solutions favor combined maneuvers, and, according to Eq. (9), the first impulse Δv_a is written as

$$\Delta v_a = \sqrt{\left(s_x x\right)^2 + \left(s_y y\right)^2 + \left(s_z z\right)^2} \tag{15}$$

Note that there are no constraints on the ranges of s_x, s_y, s_z, and the values for semi-major axis and inclination changes may be larger than unity (or may be negative), in order to take advantage of the J2 effect to reduce RAAN differences. This case generally occurs when the required RAAN change is too large, as the allowed transfer time is not sufficiently long.

The control on semi-major axis and inclination given by the first impulse, as shown by Eq. (4), leads to a change of RAAN rate during the transfer time $t = t_{k+1} - t_k$ for the chaser, and therefore causes additional RAAN change according to Eq. (12)-(14)

$$\Delta x = -m s_y y - n s_z z \tag{16}$$

which must be added to the effect of the impulses. The coefficients $m = \left(7\dot{\Omega}_0\right)\sin i_0 t$, $n = \left(\dot{\Omega}_0 \tan i_0\right)\sin i_0 t$ are obtained using Eqs. (4), (13), (14), where $\dot{\Omega}_0$ is the average RAAN rate of the chaser and the target. When the first impulse is optimized, the new RAAN rate tends to produce a smaller final RAAN difference and lower propulsive transfer cost.

The second impulse Δv_b must satisfy the conditions for the target orbit and its magnitude becomes

$$\Delta v_b = \sqrt{\left(x - s_x x - \Delta x\right)^2 + \left(y - s_y y\right)^2 + \left(z - s_z z\right)^2} \tag{17}$$

The total $\Delta v = \Delta v_a + \Delta v_b$ is

$$\Delta v_a + \Delta v_b = \sqrt{\left(s_x x\right)^2 + \left(s_y y\right)^2 + \left(s_z z\right)^2} + \sqrt{\left(x - s_x x - \Delta x\right)^2 + \left(y - s_y y\right)^2 + \left(z - s_z z\right)^2} \tag{18}$$

It is difficult to find the minimum of $\Delta v = \Delta v_a + \Delta v_b$ in closed form. Through revisiting to classical Minimum-Inclination Maneuvers by Vallado [14], an analytic approximation becomes available by squaring the two velocities to remove the square roots:

$$\Delta v_a^2 + \Delta v_b^2 = \left(s_x x\right)^2 + \left(s_y y\right)^2 + \left(s_z z\right)^2 + \left(x - s_x x - \Delta x\right)^2 + \left(y - s_y y\right)^2 + \left(z - s_z z\right)^2 \tag{19}$$

Notice that this approximation ignores the cross product terms $\left(2\Delta v_a \Delta v_b\right)$. This allows one to differentiate this expression with respect to s_x, s_y, s_z and set the derivatives to zero to find the minimum value:

$$\frac{\partial\left(\Delta v_a^2 + \Delta v_b^2\right)}{\partial s_x} = 4x^2 s_x - 2mxys_y - 2nxzs_z - 2x^2 = 0 \tag{20}$$

$$\frac{\partial\left(\Delta v_a^2 + \Delta v_b^2\right)}{\partial s_y} = -2mxys_x + \left(4y^2 + 2m^2 y^2\right)s_y + 2mnyzs_z - 2y^2 + 2mxy = 0 \tag{21}$$

$$\frac{\partial\left(\Delta v_a^2 + \Delta v_b^2\right)}{\partial s_z} = -2nxzs_x + 2mnyzs_y + \left(4z^2 + 2n^2 z^2\right)s_z - 2z^2 + 2nxz = 0 \tag{22}$$

The unknowns s_x, s_y, s_z can be obtained from Eqs. (20)-(22) as follows

$$s_x x = \frac{2x + my + nz}{\left(4 + m^2 + n^2\right)} \tag{23}$$

$$s_y y = -\frac{2mx - \left(4 + n^2\right)y + mnz}{\left(8 + 2m^2 + 2n^2\right)} \tag{24}$$

$$s_z z = -\frac{2nx + mny - \left(4 + m^2\right)z}{\left(8 + 2m^2 + 2n^2\right)} \tag{25}$$

By substituting Eqs. (23)-(25) into Eq. (18), the minimum Δv required can be simply approximated. Note that the fractions *s* may not be defined when the corresponding variable (either *x*, or *y*, or *z*) is zero, but Eqs. (23)-(25) still provide a meaningful expression for the impulse.

An important observation can be obtained in the estimated solution. By using s_x, s_y, s_z from Eqs. (23)-(25) to evaluate the cost of changing RAAN, one can easily prove that

$$s_x x = x - s_x x - \Delta x \tag{26}$$

which shows that the first and last impulse always provide the same change of RAAN. Equation (26) can be inserted into Eq. (17) to further simplify the estimation expression. As a special case, when s_x is zero (i.e., $2x = -my - nz$), one easily obtains that both s_y, s_z are equal to ½, by substituting Eq. (23) into Eqs. (24) and (25). Eq. (26) implies that $x = \Delta x$ if $s_x = 0$, which means that RAAN is not controlled by thrust but rather matched by using only the perturbation effect generated by the changes of inclination and semi-major axis.

For small eccentricity variations, the required velocity change is given by

$$\Delta v_e = \frac{1}{2} v_0 \sqrt{\Delta e_y^2 + \Delta e_x^2} \tag{27}$$

where the non-singular equinoctial elements are used for eccentricity, i.e., $e_y = e\sin\omega$, $e_x = e\cos\omega$. An empirical relation, which assumes that the Δv for the change of eccentricity vector is divided equally between each impulse and is perpendicular to Δv_a and Δv_b, is introduced to account for the additional cost of eccentricity change:

$$\Delta v' = \sqrt{\Delta v_a^2 + \left(0.5\Delta v_e\right)^2} + \sqrt{\Delta v_b^2 + \left(0.5\Delta v_e\right)^2} \tag{28}$$

which provides an eccentricity correction on the previous equation $\Delta v = \Delta v_a + \Delta v_b$.

IV. Results

The ninth edition of the global trajectory optimization competition GTCO9 [16] proposed a problem that concerned the removal of 123 debris objects. A complete summary of the winner solution of the GTOC9 problem by JPL can be found in Ref. [12]. Table 1 and 2 show the transfer durations and Δv cost for each mission. Due to the stringent time constraints of the proposed problem, the opportunity of performing optimal-time transfers was extremely rare, and limited time solutions were sought. JPL's solution is here used to evaluate the accuracy of the proposed Δv estimation method for time-limited transfers.

As described in JPL's paper, their method was very good at making large numbers of significant changes to existing solutions, but it had difficulty in finding truly global optima probably due to the existence of multiple

locally optimal solutions. Therefore, the exact solutions given in Table 2 may not guarantee the minimum, and it could be expected that the exact solution may have room to be improved to some extent.

Table 1. Transfer Duration Characteristics of JPL's solution

Mission	Number of legs	Transfer Duration, days
1	13	24.86,24.98,22.42,24.99,0.29,10.63,25.00,2.70,1.51,1.41,24.67,24.31,5.86
2	11	24.93,0.28,0.73,0.39,17.07,1.61,22.42,2.39,15.88,24.97,2.49
3	20	14.16,24.94,2.87,8.10,9.00,23.13,23.09,23.09,22.83,24.98,24.98, 24.93,24.94,9.10,13.44,24.99,24.94,24.99,24.98,24.96
4	10	23.96,6.48,16.72,23.97,23.95,23.95,23.96,23.99,23.94,23.96
5	13	0.45,3.17,24.93,10.34,12.53,7.11,13.44,24.94,24.94,24.98,22.19,24.99,22.01
6	9	24.91,0.30,18.39,3.08,20.24,24.96,24.85,24.97,0.28
7	9	15.69,0.50,9.83,24.94,24.90,24.48,20.87,24.91,0.66
8	8	10.03,24.00,2.83,24.99,24.99,24.96,21.19,24.98
9	11	22.69,4.24,24.47,24.46,24.47,24.44,24.46,24.46,24.46,18.54,9.22
10	9	0.81,11.59,7.66,1.11,17.46,6.47,20.47,24.47,3.99

Estimations and actual values are usually in good agreement (the average error magnitude is 4.37%), as shown in Table 3. A synoptic view of the missions is provided in Fig. 1, which compares actual and estimated rendezvous Δv. When the additional eccentricity correction is taken into account, the estimated solution becomes even closer to the exact solution with an average error magnitude of 2.83%, as shown in Fig. 2 and Table 4. However, in most cases the estimated solution is slightly below the corresponding exact one. It is worth noting that phasing constraints, which may affect the legs of the optimal GTOC9 solution, are not considered in the approximate analysis. An additional estimation performance for all the 113 transfer legs (where 123 debris and 10 launches are involved) is measured by the mean absolute error (MAE), which is 16.5 m/s and 13.3 m/s for cases without and with eccentricity correction, respectively.

The presented approximation method proves to be vastly superior in terms of accuracy to other commonly used approximation methods (their relative errors are even up to 20% [11]). Although machine learning methods have a computational speed advantage over traditional optimization methods, considerable computation effort is still required. It is worth noting that, in general, only analytic approximations of leg cost suit to the time-demanding but widely-used evolutionary optimization methods for targets sequence selection.

Table 2. Mission ΔV Characteristics of JPL's solution

Mission	Number of legs	ΔV, m/s	Total ΔV, m/s
1	13	161.8,139.2,65.8,208.2,115.2,300.1,564.9,78.3,105.0,233.3,453.5,340.4,300.8	3066.5
2	11	659.0,301.1,252.1,143.8,146.8,68.6,40.6,84.2,105.3,448.5,148.0	2398.0
3	20	219.1,80.8,105.2,55.2,140.2,85.5,95.0,237.6,205.9,149.9,245.2,71.6,197.3, 160.4,132.2,240.0,161.2,364.3,230.4,232.5	3409.5
4	10	86.1,103.1,62.6,222.9,709.1,553.9,219.9,233.9,739.0,232.6	3163.1
5	13	129.6,45.2,172.9,52.6,160.7,280.8,221.1,163.5,98.2,115.7,164.8,674.8,291.1	2571.0
6	9	156.0,198.0,305.8,71.2,194.4,920.5,314.1,353.0,272.8	2785.8
7	9	400.6,173.6,211.3,374.4,109.6,171.2,145.1,194.3,233.0	2013.1
8	8	287.9,111.9,112.2,144.5,540.0,260.1,198.8,82.7	1738.1
9	11	83.3,148.1,495.9,464.9,405.2,285.9,254.8,62.3,156.6,36.5,174.9	2568.4
10	9	189.4,112.9,110.0,121.3,117.9,280.1,300.4,120.6,70.2	1422.8

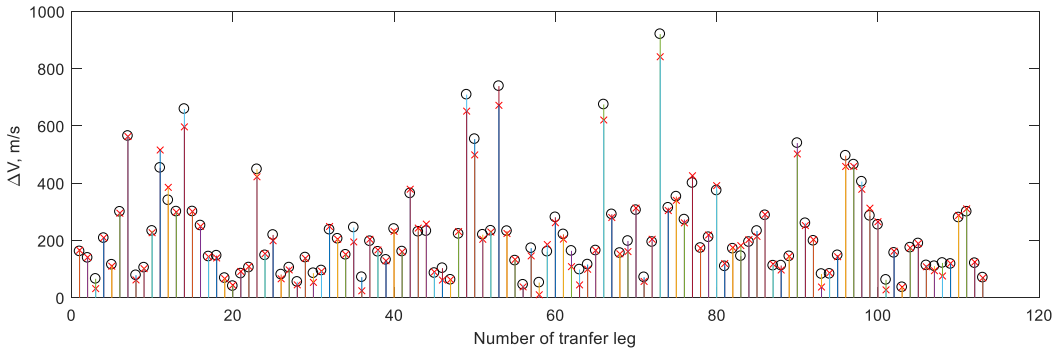

Fig. 1 Synoptic view of the comparison between exact and estimated solutions (the circle represents JPL's exact solution, and cross is the estimated solution)

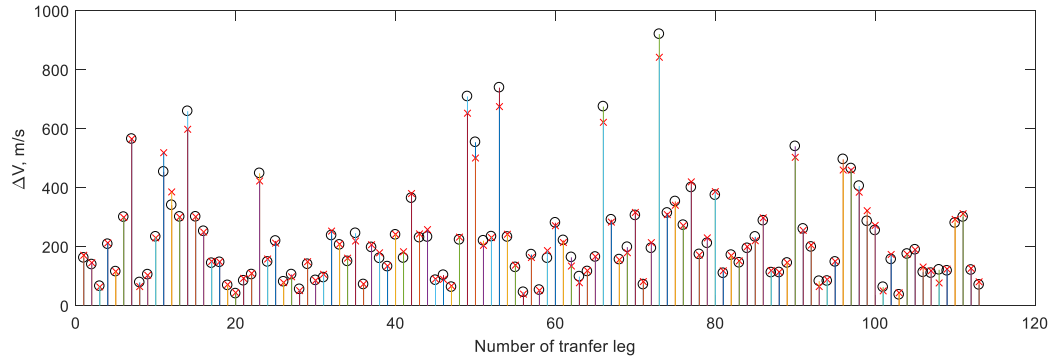

Fig. 2 Synoptic view of the comparison between exact and estimated solutions (the circle represents JPL's exact solution, and cross is the estimated solution with eccentricity correction)

Table 3. Mission ΔV by the Simple Approximation

Mission	ΔV, m/s	Total ΔV, m/s	Error,%
1	165.7,140.7,31.49,209.2,109.9,295,562.9,61.85,101.4,226.8,515.7,385.3,298.9	3104.9	**1.25**
2	596.5,300.8,249.1,142.9,138.6,66.43,43.64,91.4,108.8,422.2,153.4	2313.6	**-3.52**
3	198.7,65.82,96.87,44.67,137.4,53.34,92.44,248.6,204.2,151.2,194.6, 23.93,203.9,166.5,128.6,231.6,160.3,378.8,243,256.9	3281.3	**-3.76**
4	89.73,61.54,62.77,230.8,651.5,498.6,203.9,229.2,671.8,224.1	2924.0	**-7.56**
5	133.2,37.62,145.8,10.03,185.5,261.7,204.5,108.3,44.47,99.21,165.1,620.5,279.9	2296.0	**-10.7**
6	153.1,160.9,313,56.61,204,841.4,304.2,339.8,261.2	2634.2	**-5.44**
7	425.8,172.9,218.9,391.3,119.1,174.8,181.8,202.8,214.0	2009.3	**-0.19**
8	290.7,117,96.53,144.3,502,251.7,202.7,37.14	1642.1	**-5.52**
9	86.24,142.9,458.3,458.3,378.6,312.6,265.2,27.18,162.2,36.86,174.1	2502.5	**-2.56**
10	189.0,107.9,94.09,75.6,119.6,287.3,310.3,124.2,69.21	1377.2	**-3.20**

Table 4. Mission ΔV by the Simple Approximation with Eccentricity Correction

Mission	ΔV, m/s	Total ΔV, m/s	Error,%
1	170.5,145.1,63.13,212.2,115.4,299,564.8,64.33,102.8,229.4,518.4,385.3,300.1	3170.6	**3.39**
2	597.8,301.1,249.3,149.8,148.2,71.08,43.65,92.25,108.9,422.4,157.8	2342.3	**-2.32**
3	211.7,77.72,97.45,50.57,148.7,85.18,106,252.5,208.2,160.7,218.8, 72.93,206.2,178.8,134.1,241.5,182.4,379.8,243,257.4	3513.6	**3.05**
4	89.89,88.69,66.46,232.1,652.3,500.3,204.2,230.4,674.7,241.9	2980.9	**-5.76**
5	137.0,38.75,162.9,51.25,186.2,270.6,213.8,134,77.32,118.4,166,621.4,283.0	2460.5	**-4.30**
6	155.2,179.2,315.8,81.18,213.3,842,308.3,340.1,271.2	2706.2	**-2.86**
7	419.4,171.4,229.4,386.3,117.7,169.3,151.3,199.6,219.8	2064.3	**2.54**
8	297.4,118.5,113.6,145.7,502.7,254.9,204.8,64.43	1701.9	**-2.08**
9	88.35,149.8,459.6,459.1,384.4,321.6,271.7,49.73,173.1,43.15,174.3	2574.7	**0.25**
10	189.4,130.6,117.8,76.58,123.5,292.2,311.3,126,80.48	1447.9	**1.76**

Table 5. Detailed solution of the first leg of mission-1 (debris 23 to 55)

Solution		time, day	Δv_i, m/s	Δa, km	Δi, deg	$\Delta\Omega$, deg	RSR Δv, m/s	Total Δv, m/s
Exact	1	0.275	134.2	-37.08	-0.999	-0.083	132.2	164.55
	2	0.312	0.818	1.196	-0.0037	-0.0014	0.811	
	3	24.828	15.41	8.671	-0.114	0.005	15.56	
	4	24.860	14.12	-18.23	-0.076	0.023	14.08	
Estimated	1	0	98.17	13.59	-0.743	-0.104	98.17	165.73
	2	24.86	67.56	-59.03	-0.449	-0.104	67.56	

Table 6. Detailed solution of the first leg of mission-8 (debris 86 to 34)

Solution		time, day	Δv_i, m/s	Δa, km	Δi, deg	$\Delta\Omega$, deg	RSR Δv, m/s	Total Δv, m/s
Exact	1	0.0667	141.30	54.82	-0.778	-0.728	141.26	294.06
	2	0.102	76.75	-39.67	-0.432	-0.383	77.80	
	3	9.997	33.32	-44.15	-0.00027	-0.187	33.45	
	4	10.03	42.70	-57.10	-0.0190	-0.233	42.52	
Estimated	1	0	165.00	70.71	-1.016	-0.705	165.00	290.73
	2	10.03	125.73	-156.82	-0.213	-0.705	125.73	

Table 5 and Table 6 show two detailed solutions by comparing exact solution and estimation. The transfer time is relatively long (24.86 day) and medium (10.03 day), respectively, for the two solutions. Leg details are not given in Ref. [9], and the exact solutions are here obtained by an optimization procedure involving up to four impulses, by means of a continuous ant colony optimization (ACO) method [5]. The exact solutions by ACO are very close the JPL's exact solutions (which considered up to 5 impulses), though a slightly larger total Δv is obtained in both cases here. In the exact optimization, multiple impulses are favored in order to match phase and eccentricity, which have, however, a limited impact on the total velocity change.

The approximate two-impulse solution guarantees a good accuracy in terms of total costs. The two impulses, which are placed at the start and final time of each leg, efficiently perform the most important orbital changes (i.e., RAAN, semi-major axis, and inclination), although corresponding to a rather different strategy in terms of a, e, i, and Ω, with respect to exact solutions. For these trajectories the transfer time is not optimal, and an active change of RAAN with propulsion is needed, in addition to inclination, in order to obtain the plane alignment. This kind of maneuvers do not occur in cases where sufficient transfer time is allowed, and demonstrate that a time-limited solution is required. In the estimated solution, RAAN changes are the same between the initial maneuver and the last maneuver, as illustrated in the previous Section (i.e., Eq. (26)). It is worth noting that, for the transfer described in Table 5, the two-impulse approximation uses a different strategy in terms of semi-major axis change with a small initial increase, but is nonetheless capable of obtaining a similar overall Δv cost. In both approximate solutions the semi-major axis is initially increased and then decreased, with the purpose of obtaining the best tradeoff in terms of total Δv between changes of RAAN and other parameters (semi-major axis and/or inclination). In other cases, a similar strategy is used for inclination. This fact shows that the semi-major axis and/or inclination changes may be not monotonic, which is peculiar in this kind of J2-perturbed time-limited body-to-body transfers.

The root-sum-square (RSR) of individual Δvs required for the combined changes of the semi-major axis, RAAN, and inclination according to Eq. (9), are in good agreement with the corresponding exact Δv_i, as shown in Table 5 and 6. This fact confirms that the Δv estimation method described in Eqs. (15) and (17), which evaluates the impulses as the root-sum-square of the cost of individual changes of orbital parameters into account, works properly.

V. Conclusions

An analytic procedure has been developed for preliminary evaluation of transfer costs between objects in LEO, in order to speed up the analysis of debris removal missions aiming at multiple objects, when they must be selected in large sets of targets with similar orbit inclination. In fact, in these cases, the solution of the combinatorial problem may be impractical in terms of computational time, even though it can be carried out off-line. The analysis tool that has been developed in this paper is therefore in particular beneficial in the preliminary design phases, when mission feasibility must be assessed and trade-offs are required, and a precise evaluation of the costs can reduce design uncertainties. The good accuracy of the proposed estimation method has been verified by comparison with precisely optimized solutions, and the mean relative estimation error is below 3%. Even though the estimation is in general slightly below the exact solution, the benefits, which can be obtained when a proper analytical approximation of transfer cost is used in multiple-target active debris removal, are thus demonstrated.

References

[1] Kessler, D., Johnson, N., Liou, J.-C., and Matney, M., "The Kessler Syndrome: Implications to Future Space Operations," *Advances in the Astronautical Sciences*, Vol. 137, Univelt, San Diego, CA, 2010, pp. 47–62; also AAS Paper 10-016, 2010.

[2] Liou, J. -C., and Johnson, N. L., "Risks in Space from Orbiting Debris," *Science*, Vol. 311, No. 5759, 2006, pp. 340-341. doi: 10.1126/science.1121337

[3] Liou, J.-C., Johnson, N., and Hill, N., "Controlling the Growth of Future LEO Debris Populations with Active Debris Removal," *Acta Astronautica*, Vol. 66, Nos. 5–6, 2010, pp. 648-653. doi:10.1016/j.actaastro.2009.08.005

[4] Cerf, M., "Multiple Space Debris Collecting Mission--Debris Selection and Trajectory Optimization," *Journal of Optimization Theory and Applications*, Vol. 156, 2013, pp. 1234–1258. doi:10.1007/s10957-012-0130-6

[5] Shen, H.-X., Zhang, T.-J., Casalino, L., and Patrone, D., "Optimization of active debris removal missions with multiple targets," *Journal of Spacecraft and Rockets*, Vol. 55, No. 1, 2018, pp. 181-189. doi: 10.2514/1.A33883

[6] Bang, J., and Ahn, J., "Multitarget Rendezvous for Active Debris Removal Using Multiple Spacecraft," *Journal of Spacecraft and Rockets*, Vol. 56, No. 4, 2019, pp. 1237-1247. doi: 10.2514/1.A34344

[7] Li, H., Chen, S., and Baoyin, H., "J2-Perturbed Multitarget Rendezvous Optimization with Low Thrust," *Journal of Guidance, Control, and Dynamics*, Vol. 41, No.3, 2018, pp. 796-802. doi: 10.2514/1.G002889

[8] Alfriend, K. T., Lee, D.-J., and Creamer, N. G., "Optimal Servicing of Geosynchronous Satellites," *Journal of Guidance, Control, and Dynamics*, Vol. 29, No. 1, 2006, pp. 203–206. doi:10.2514/1.15602

[9] Izzo, D., Martens, M., and Pan, B., "A survey on artificial intelligence trends in spacecraft guidance dynamics and control," *Astrodynamics*, Vol. 3, 2019, pp. 287-299. doi: 10.1007/s42064-018-0053-6

[10] Li, H., Chen, S., Izzo, D., and Baoyin, H., "Deep networks as approximators of optimal low-thrust and multi-impulse cost in multitarget missions," *Acta Astronautica*, Vol. 166, 2020, pp. 469-481. doi: 10.1016/ j.actaastro.2019.09.023.

[11] Zhu, Y., Luo, Y., "Fast Approximation of Optimal Perturbed Long-Duration Impulsive Transfers via Deep Neural Networks", 2020, arXiv:1902.03741 [math.OC]

[12] Petropoulos, A. E., Grebow, D., and Jones, D., et al., "GTOC9: Methods and results from the Jet Propulsion Laboratory team," *Acta Futura*, No. 11, 2018, pp. 25-35. doi: 10.5281/zenodo.1142857

[13] Vallado, D. A., and Crawford, P., "SGP4 Orbit Determination," *AIAA/AAS Astrodynamics Specialist Conference*, 2008, paper AIAA-2008-6770. doi: 10.2514/6.2008-6770

[14] Vallado, D. A., Fundamentals of astrodynamics and application. Springer Science & Business Media, 2001.

[15] Edelbaum, T. N., "Propulsion Requirements for Controllable Satellites," *ARS Journal*, Vol. 31, No. 8, 1961, pp. 1079–1089. doi:10.2514/8.5723

[16] Izzo, D., and Martens, M., "The Kessler Run: On the Design of the GTOC9 Challenge," *Acta Futura*, No. 11, 2018, pp. 11–24. doi: 10.5281/zenodo.1142857